



Contents lists available at ScienceDirect

The Journal of Supercritical Fluids

journal homepage: www.elsevier.com/locate/supflu



Effect of additives on the properties of silica based aerogels synthesized from methyltrimethoxysilane (MTMS)

Luisa Durães*, Ana Maia, António Portugal

CIEPQPF, Department of Chemical Engineering, Faculty of Sciences and Technology, University of Coimbra, Pólo II, Rua Sílvio Lima, 3030-790 Coimbra, Portugal

ARTICLE INFO

Article history:

Received 18 February 2015

Received in revised form 16 June 2015

Accepted 19 June 2015

Available online xxxx

Keywords:

Sol-gel

MTMS-derived aerogel

Network modifier

Poly(ethylene glycol)

Bis(trimethoxysilyl) hexane

Trimethoxy(octadecyl)silane

ABSTRACT

Aerogels are regarded as one of the most effective thermal insulation materials. Starting from methyltrimethoxysilane (MTMS) as sol-gel precursor, the supercritically dried silica based aerogels exhibit very low density and thermal conductivity, high hydrophobicity and remarkable flexibility, meeting the requirements for weight-sensitive insulation applications, e.g. for Space environments. However, further improvement in the properties of MTMS-derived aerogels may be achieved by using small amounts of additives/network modifiers in the synthesis. In this work, poly(ethylene glycol) (PEG), bis(trimethoxysilyl) hexane (BTMSH) and trimethoxy(octadecyl) silane (ODS) were investigated for this purpose. Whereas PEG allows for manipulation of the pore size distribution, leading to a decrease in bulk density of the aerogel, BTMSH reinforces the gel structure links, increasing its homogeneity and cohesion and reducing the dust release. The effect of the long length of alkyl substituent group of ODS resulted on an increased flexibility and reduction of particle shedding of the aerogels.

© 2015 Elsevier B.V. All rights reserved.

1. Introduction

Silica aerogels, which are obtained by sol-gel technology followed by supercritical fluids drying, exhibit exceptional properties that can make them potential competitor materials for high performance insulators used in Space environments. In fact, they were already used as capture medium for hypervelocity cosmic particles (in Stardust) and as thermal insulators for Mars exploration (Mars Pathfinder, Mars Rovers, Mars Science Lander) [1]. However, whereas native silica aerogels are very brittle and deteriorate over time upon exposure to moisture, the MTMS-derived aerogels do not show these weaknesses due to their high flexibility and hydrophobicity [2–5]. The later exhibit very low bulk density ($\sim 50 \text{ kg m}^{-3}$) and thermal conductivity (achieving $0.036 \text{ W m}^{-1} \text{ K}^{-1}$), high porosity ($> 95\%$) and surface area ($\sim 500 \text{ m}^2 \text{ g}^{-1}$), good flexibility (order of kPa) and high hydrophobic character ($\sim 140^\circ$) [5,6]. Despite these satisfactory results, further improvements towards a decrease in density and thermal conductivity and an increase in the mechanical strength and integrality may be attempted by addition of certain network modifiers to the starting precursor system. This would allow to widen the possible

Space applications of these materials, as well as other non-Space applications.

It is also important to note that the MTMS-derived aerogels structure is mainly inorganic and this feature gives them good thermal stability and avoids the glass transition phenomenon, which may not be the case for polymer-reinforced silica aerogels [2]. Thus, in order to maintain the referred characteristics of MTMS-derived aerogels, in this work, the chemical modifications of the aerogels network were restricted to the addition of small quantities of additives or co-precursors, as they introduce organic moieties in the system (besides the already existing methyl groups). Poly(ethylene glycol) (PEG), bis(trimethoxysilyl) hexane (BTMSH) and trimethoxy(octadecyl) silane (ODS) were the chosen additives, for the reasons described below. To the best of our knowledge, these additives were not yet tested in the MTMS precursor system.

The influence of PEG additive was investigated, as it is known as a porogen which allows manipulating the pore size distribution [7] and, consequently, it can lead to a decrease in the bulk density of the aerogels. On the other hand, when samples in a semi-industrial scale are needed, the reinforcement of the gel structures is crucial. Thus, the co-precursor BTMSH was tested with the purpose to check its effect like a bridging organic ligand on the connectivity of the silica network and, consequently, in some important properties of the aerogels like their mechanical strength and integrality. Also the effect of ODS, with a long alkyl chain (18C), was used try-

* Corresponding author. Fax: +351 239798703.

E-mail address: luisa@eq.uc.pt (L. Durães).

Table 1

Synthesis conditions and gelation time of MTMS-derived gels, with and without additives.

Sample	Acid solution concentration (M)	Basic solution concentration (M)	Solvent/MTMS (molar ratio)	Additive type and amount (molar ratio)	Gelation time (h)
A	0.01	10	35	–	4–5
A-PEG	0.01	10	35	PEG600/MTMS = 0.01	~5
B	0.1	10	25	–	~2
B-BTMSH	0.1	10	25	BTMSH; 2% of Si	~1
B-ODS	–	10	25	ODS; 2% of Si	~2

ing to improve, mainly, the integrity of the larger MTMS-derived aerogels.

BTMSH and ODS precursors were already tested by Tan and Rankin [8] and Brambilla et al. [9], respectively, but never combined with MTMS. In the first case, the aim was to study how changes in silanes or orthosilicates chemical structure (tetramethylorthosilicate – TMOS, MTMS, BTMSH, ODS and others) affected the gelation and properties of the obtained organosilicas, when using the precursors separately. Brambilla et al. prepared octadecylsilane-modified silicas by grafting and sol-gel methods based on tetraethylorthosilicate (TEOS) precursor.

In the present work, the viability of gel formation for larger samples was also assessed as well as the release of dust from aerogels, which are critical issues for using these materials in space technologies.

2. Material and methods

2.1. Synthesis procedure

The silica precursor in the syntheses was MTMS (98% Aldrich) and the tested chemical additives were PEG 600, BTMSH and ODS. Methanol (99.9% Aldrich), oxalic acid (99%, Fluka) and ammonium hydroxide (25% in H₂O, Aldrich) were used as solvent, acid catalyst and basic catalyst, respectively. The samples, except the ODS ones, were obtained by a two-step acid-base catalysed sol-gel process already described by Durães et al. [5] and inspired in the approach proposed by Rao et al. [10]. Briefly, MTMS is diluted in methanol and then oxalic acid is added to promote the hydrolysis of the precursor. The ammonium hydroxide solution is added after 24 h, giving rise to the condensation of the silanols and forming a sol, which turns to a gel in the period of time given in Table 1 (see gelation time). The molar ratios of MTMS:methanol:acidic water:basic water were 1:35:4:4, in the system with PEG, and 1:25:4:4 in the system with BTMSH. PEG and BTMSH were added in the hydrolysis stage, together with MTMS.

The gel with ODS was prepared in just one step catalysed by base (one-pot), inspired in the procedure proposed by Anderson et al. [11], whom prepared native silica materials derived from TMOS precursor with this approach. The ODS was mixed with methanol and MTMS, and then the basic water was added, under stirring. The molar ratios of MTMS:methanol:basic water were 1:25:8.

The PEG/MTMS molar ratio was equal to 0.01 and the percentages of BTMSH and ODS were 2% of Si, amounts that were optimized previously considering the compromise of not increasing much the bulk density of the materials. The monolithicity was also recognized as a crucial criterion; amounts of additives at or above a PEG/MTMS molar ratio of 0.05 and 5% of Si derived from ODS or BTMSH led to broken samples.

Samples A and A-PEG were prepared in test tubes and the remaining samples, B, B-BTMSH and B-ODS were prepared in petri dishes (three times the volume of the test tubes), using the differentiated conditions summarized in Table 1.

After aging, the samples were dried by a continuous Low Temperature Supercritical Fluids Drying (LTSCD) stage using CO₂ as supercritical solvent, with a layout/strategy similar to an older sys-

tem already applied by the authors in an earlier work [12]. The new system was designed and built by *Paralab* (Portugal) and consists of several parts, namely: (i) the liquid CO₂ feeding part, with a CO₂ bottle and a cooling bath; (ii) two pumps for the pressurization of liquid CO₂ and organic solvents; (iii) a 50 cm³ stainless steel extraction cell to contain the sample; (iv) an oven, to increase the temperature above the critical temperature of CO₂ (31 °C); (v) a flow meter and several regulating valves and pressure transducers, for pressure and flow measuring/regulation; (vi) a back-pressure regulator, to stabilize pressure; (vii) an acquisition and automatic control system for registry and following/setting the pressurization/depressurization stages and flow conditions.

The applied LTSCD procedure consisted in two steps, the first being the washing of the sample by passing the solvent in the extraction cell at 100–150 bar, in order to remove the water and catalysts (and also PEG), and the second is the drying itself, carried out by continuously pumping supercritical CO₂ to extract methanol by its dissolution in scCO₂. The drying took place at 50 °C and 150–200 bar. The used operating conditions were optimized to obtain less dense materials.

2.2. Characterization methods

Several techniques were used for the physicochemical/structural, thermal and mechanical characterization of the aerogels.

The chemical structure of the aerogels was assessed by FTIR (FT/IR-4200 spectrometer, Jasco) and their elemental analysis was performed using a Fissions Instruments model EA 1108CHNS-O apparatus. The FTIR spectra were collected using the KBr pelletting method, with a wave number interval of 400–4000 cm⁻¹ and averaging 64 scans. The pellets were prepared by milling and mixing 80 mg of KBr and 0.2–0.3 mg of aerogel. The applied resolution was 4 cm⁻¹. The mass percentages of CHN elements were obtained by dynamic flash combustion of tin capsules with 2–3 mg of aerogel, maintaining the oven of the elemental analysis equipment at 900 °C (Pregl-Dumas method), with a flow of oxygen (99.995%) enriched He (99.995%). After quantitative conversion in two catalyzed stages of oxidation-reduction, the resultant gases are separated and detected in a chromatographic column (Porapak QS) and a thermal conductivity detector (TCD), respectively. The evaluation of O element was performed by the Unterzaucher modified method, based on the pyrolysis of silver capsules with 2–3 mg of aerogel, at 1060 °C, in pure He (99.995%), followed by removal of interfering gases in ascarite and anhydronite packings, separation of the gases in a molecular sieve (5 M) GC column and, finally, detection by a TCD.

The contact angle of water in the samples was evaluated by a Contact Angle System OCA 20, from Dataphysics, in order to access the hydrophobicity of the aerogels. For this purpose, water drops of 10 µl were dropped over horizontal and flat surfaces of the aerogel. The contact angle was measured directly from the obtained photograph of the water drop and its contour fit. Ten valid measurements were averaged to obtain the final values and uncertainties (95% confidence interval).

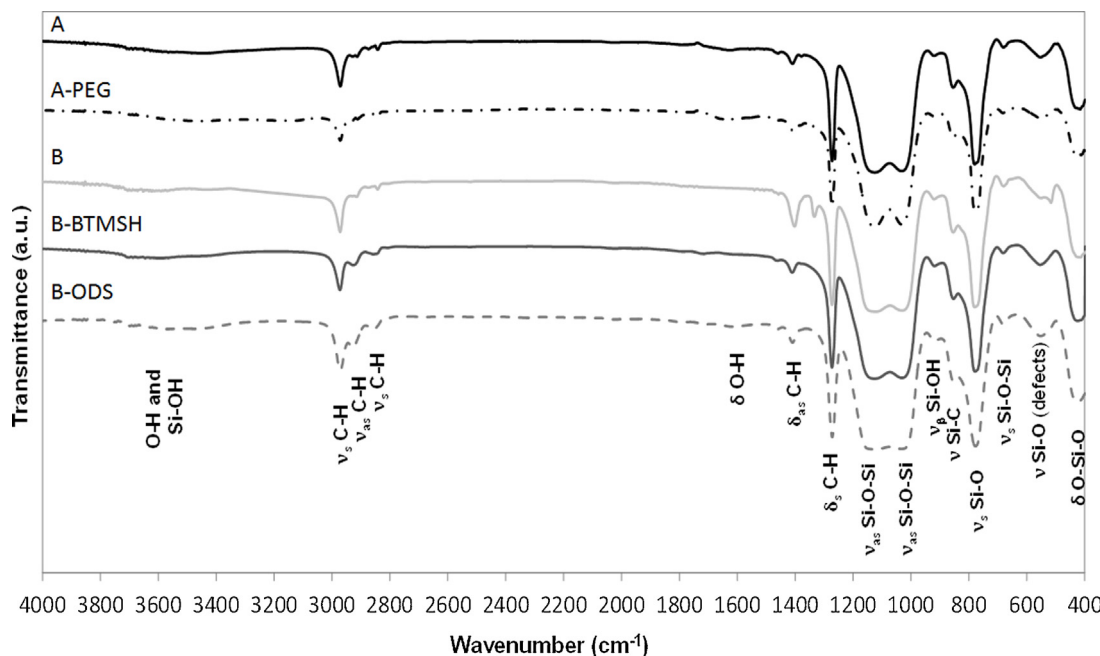


Fig. 1. FTIR spectra of the MTMS-derived aerogels with and without additives (v – stretching vibration, v_s – symmetric stretching vibration, v_{as} – asymmetric stretching vibration, v_β - in-plane stretching vibration, δ – deformation vibration, δ_s – symmetric deformation vibration (bending), δ_{as} – asymmetric deformation vibration (bending)).

The bulk density was determined by the ratio mass/volume of regular pieces (parallelepipeds) of aerogel (4 pieces of each of the 3 aerogels replicas), with uncertainty evaluated by the 95% confidence interval. An electronic digital micrometer and an analytical balance were used for this purpose. The skeletal density of the aerogels was also measured with He picnometry (Accupic 1330, Micromeritics), in order to evaluate the porosity of the samples – $(1 - \rho_b/\rho_s) \times 100$ (ρ_b – bulk density; ρ_s – skeletal density). For skeletal density, the samples were placed in the sample cell, which was pressurized to ~ 1.25 bar above the ambient pressure and allowed to reach equilibrium. From the difference of pressure between the sample cell and reference cell, over 5 runs, the actual volume of the sample skeleton was calculated (always with a SD lower than 10%).

Specific surface area and the pore size distribution of the materials were determined by using nitrogen gas adsorption/desorption isotherms, which were obtained with a Micrometrics ASAP 2000 analyzer. Before analysis, the aerogel samples were degassed in an oven during 3 days in vacuum at 50°C , and, subsequently in the analyser, at 200°C in vacuum, for 24 h, to remove adsorbed species. In the analysis, volumes of the adsorbed nitrogen at several different relative pressures (0.05–0.3) were taken at 77 K to evaluate the specific surface area by the BET theory. Standard deviation values were evaluated for these estimates. The desorption isotherm was used (relative pressures from 1 to 0.5) to assess the pore size distribution by the BJH model. The lower and upper limits for the pore diameters were 1.7 nm and 300 nm, respectively.

The microstructure of the samples was observed by scanning electron microscopy – SEM (JMS-5310, JOEL). The samples were previously coated with a layer of vapor-deposited Au, because the aerogels presented high electrical resistivity. This was performed in a Physical Vapour Deposition (PVD) chamber, for 30 s. The SEM operating work distance, voltage and current was adjusted in each case to obtain better contrast and resolution of the images.

The Thermal Constants Analyzer TPS 2500 S, from Hot Disk, was used to obtain the thermal conductivities of aerogels at several temperatures. The sensor was clamped between two cylindrical pieces of the sample (diameter of 1.5 cm and thickness larger than 0.5 cm) and was then heated by a constant electrical current for a short

period of time. The generated heat dissipated from the sensor into the surrounding sample material, causing a rise in temperature of the sensor and surrounding sample material (transient method). The obtained temperature profiles were mathematically treated to obtain the thermal properties of the material. The used equipment has reproducibility better than 1% and accuracy better than 5%.

The modulus of elasticity of the samples was assessed through a uniaxial compression test. This test was carried out in a Shimadzu AG-IS 100KN device, equipped to control the compression velocity, and a AND EK-1200i balance. The data collected for each test was converted into a stress-strain curve, being the Young's modulus and the elongation at break obtained from these curves, from the slope of the elastic region and x-axis value of the final point, respectively.

The thermal behaviour of the aerogels was evaluated by thermogravimetric analysis (TGA), using a SDT-Q600 model, from TA Instruments. The samples were placed in an alumina pan and heated from room temperature to 1200°C , at a constant rate of $10^\circ\text{C}/\text{min}$, under pure nitrogen (99.995%) flow (10 mL/min).

Finally, a visual inspection was performed to evaluate the release of dust (white) from the aerogels, using a black paper as background contrast. Small parallelepipeds of the materials with the same dimension/shape (with perfectly flat bottom surface) were cut from freshly prepared materials; these were dragged twice on the black paper, in order to inspect and photograph the powder trace of each sample.

3. Results and discussion

The analysis of the physicochemical/structural, thermal and mechanical properties of the aerogels synthesized with additives was made taking as references the aerogels synthesized only with MTMS for the two different synthesis conditions (samples A and B from Table 1).

3.1. Chemical characterization

3.1.1. FTIR

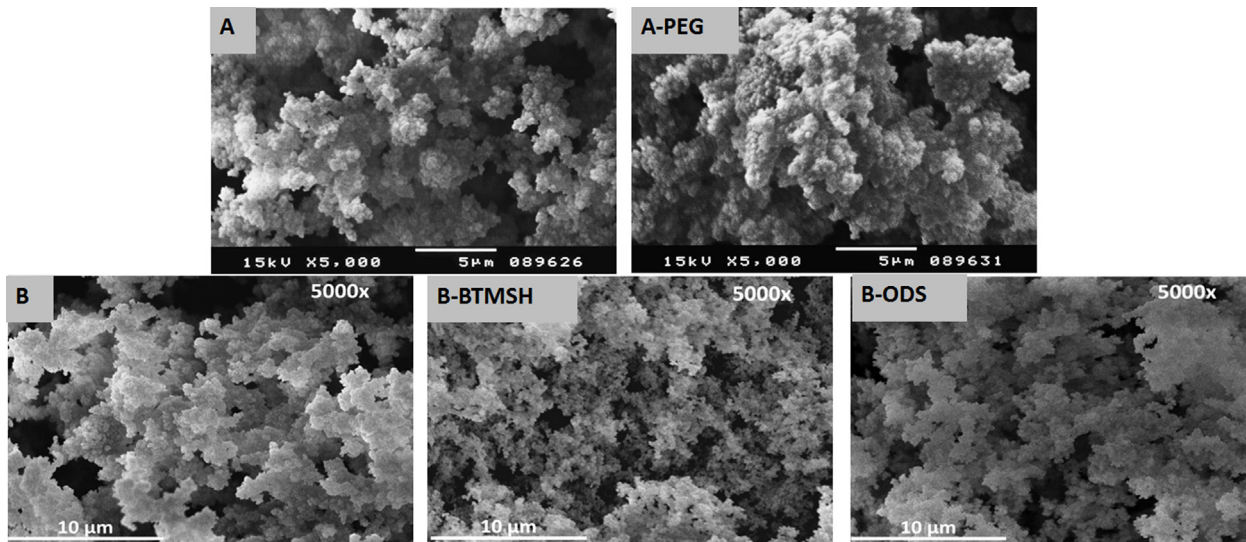
Fig. 1 shows the typical FTIR spectra obtained for the synthesized aerogels, in which it is possible to observe several bands

Table 2

Elemental analysis (EA) and contact angle results.

Sample	EA (experimental) ^a				EA (theoretical)		Contact Angle (°)
	wt% C	wt% H	wt% O	wt% N	wt% C compl.	wt% C incompl.	
A	18.15	4.67	1.21	0.08	17.9	15.8	147 ± 4
A-PEG	22.10	4.78	0.75	0.47	23.5	21.1	146 ± 4
B	18.76	4.84	0.74	0.37	17.9	15.8	140 ± 4
B-BTMSH	19.11	4.97	0.75	0.16	18.5	16.3	145 ± 8
B-ODS	20.69	4.98	1.3	0.04	22.4	19.9	150 ± 5

^a The wt% errors associated with the measurements are ±0.40, ±0.20, ±0.25 and ±0.15, for C, H, N and O, respectively; Two concordant replicas were run.

**Fig. 2.** SEM images for the MTMS-derived aerogels with and without additives.

that were ascribed to the various bond vibrations considering the related literature [13,14].

The obtained FTIR spectra are similar in what concerns the observed types of bonds and intensity of absorptions and are in agreement with the expected chemical bonds in the MTMS-derived aerogels: a predominant inorganic network composed by Si—O—Si bonds (silica) with a methyl group per silicon and hydroxyl groups at the network ends.

For the five samples, the main peak at ~770 cm⁻¹ and the large and intense bands between 1000 cm⁻¹ and 1150 cm⁻¹ are due to symmetric and asymmetric stretching vibrations of Si—O—Si bonds, respectively. Near 420 cm⁻¹ appears the bending mode of the same bonds. At ~550 cm⁻¹, it is possible to note the Si—O stretching of the SiO₂ network defects. The existence of methyl groups in the structure is confirmed by the symmetric and asymmetric stretching vibrations of the C—H bonds that are found between 2800 and 3000 cm⁻¹ and the stretching vibrations of the Si—C bonds at ~850 cm⁻¹. The symmetric and asymmetric deformation vibrations of C—H bonds are observed at ~1270 cm⁻¹ and ~1400 cm⁻¹, respectively. The overlapping of the O—H stretching bands of hydrogen-bonded adsorbed water and Si—OH stretching of surface silanols are represented by a broad and very weak band for all samples at ~3400 cm⁻¹, demonstrating a good extent of the condensation reactions (residual Si—OH groups) and a high hydrophobic character. The absorption corresponding to the deformation vibration of the O—H bonds appears just after 1600 cm⁻¹.

The presence of the additives is not remarkably perceptible because of the small quantity used in the synthesis of the aerogels, although BTMSH and ODS additives are contributing to a slight increase of intensity of the previously identified C—H bonds between 2800 and 3000 cm⁻¹. PEG additive seems to have been removed by the washing step in the drying stage, as there are no

differences between the A-PEG and A samples spectra. The characteristic PEG band, relative to C—O—C bonds, at 1100 cm⁻¹ [14] may be hidden by the Si—O—Si stretching vibrations, but no signs of more intense bands due to OH terminal groups of PEG are noticed.

3.1.2. Elemental analysis

Table 2 presents the results of the mass percentages of C, H, O and N obtained by elemental analysis. The residual contamination by the remaining basic catalyst, although small (<0.5 wt%), is noticed by the presence of nitrogen. Considering that complete condensation of the silanols occurs and neglecting the OH terminal groups of the network, the estimated elemental ratios for the pure MTMS-derived aerogels, in a wt% basis, are 41.8Si: 35.8O: 17.9C: 4.5H. The very low experimental values for the wt% O in the samples can be explained by the temperature of the equipment furnace (1060 °C), which is not high enough to break the Si—O bonds. In the case of H, the OH terminal groups contribute to have higher experimental values than the theoretical ones. Thus, only the percentage of C will be considered for further comparison. In this way, theoretical calculations were made to evaluate the expected wt% of C for complete and incomplete (one OH per Si) condensation, for the average structural units obtained in the systems tested in this work (**Table 2**).

Given that the estimated wt% C for incomplete condensation is lower than for complete condensation, the obtained experimental values for the samples without additives are in good agreement with the theoretical hypothesis of complete condensation. The difference between the estimated and the experimental values (slightly higher) are due to the presence of impurities. This is also the case for the aerogel with BTMSH, but with a higher wt% of C, both for experimental and theoretical values, due to the presence of hexyl groups. In the case of the sample A-PEG, it is observed

Table 3

Bulk densities, porosities, surface areas, thermal conductivities and modulus of elasticity of the MTMS-derived aerogels.

Samples	Bulk density (kg m^{-3})	Porosity (%)	BET surface area ($\text{m}^2 \text{g}^{-1}$)	Thermal Conductivity ($\text{W m}^{-1} \text{K}^{-1}$)			Modulus of elasticity (kPa)
				-25 °C	20 °C	125 °C	
A	48.8 ± 1.9	96	256.9 ± 6.0	0.031	0.037	0.045	3.3
A-PEG	41.7 ± 1.1	97	177.0 ± 4.5	0.030	0.036	0.043	3.2
B	53.1 ± 4.9	96	324.1 ± 4.7	0.032	0.039	0.042	7.9
B-BTMSH	61.8 ± 8.7	96	325.8 ± 5.6	0.033	0.038	0.043	8.6
B-ODS	59.4 ± 2.8	94	357.0 ± 6.5	0.032	0.036	0.046	3.1

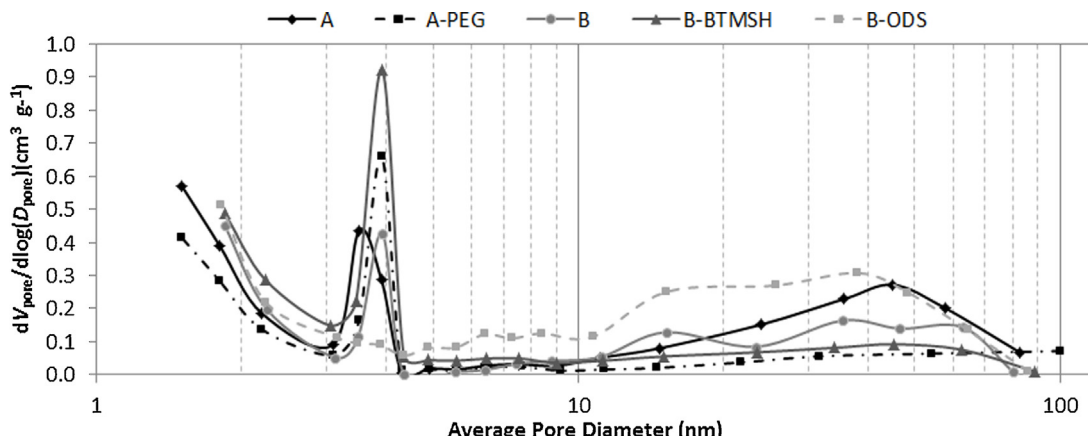


Fig. 3. Pore size distributions, obtained by nitrogen desorption, for the MTMS-derived samples with and without additives.

that part of the additive has been removed by washing in the drying stage, if complete condensation is considered. For the sample with ODS, the experimental wt% of C is more in agreement with the hypothesis of incomplete condensation, and this may be due to the steric hindrance caused by the long alkyl chain.

3.1.3. Contact angle

The obtained contact angle values for the studied aerogels (Table 2) are between ~ 140 and 150° . These values are very high, proving the high hydrophobic character of the synthesized aerogels, which is provided by the presence of the non-polar methyl groups ($\text{Si}-\text{CH}_3$) attached to Si. The presence of ODS, with the long non-polar chain, increases the hydrophobic character of the aerogels. Also BTMSH has a slight positive effect on the hydrophobicity of the aerogel. It is worth mention that the hydrophobic nature of the aerogel is very important to avoid its deterioration with environmental humidity and to maintain the aerogel cleanliness (self-cleaning feature).

3.2. Physical/structural characterization

3.2.1. SEM

The SEM micrographs of the studied samples (Fig. 2), with a magnification of $5000\times$, show that the aerogels microstructure grew in 3D, with a diffuse and foam-like structure composed by small interlinked units ($\ll 1 \mu\text{m}$). In general, as expected for such low bulk density materials, the images of the MTMS-derived aerogels show structures with a highly ramified pattern, and the presence of small pores (below $1 \mu\text{m}$), as well as quite large pores (of some micrometers or above) – meso and macropores. It is not possible, with the attained resolution, to verify the presence of micropores.

Comparing the two samples made in test tubes (A and A-PEG), the sample with lower bulk density (see Table 3 presented in Section 3.2.2), i.e., A-PEG, shows larger holes (macropores) in its structure. This may be due to the spaces created by the removal of PEG from the network during the washing stage. Moreover, more regular clusters are observed in the sample with PEG.

The three samples prepared in petri dishes seem to have a more uniform and closed network, in agreement with the higher densities of these materials. In addition, samples B-BTMSH and B-ODS show a less agglomerated pattern, particularly noticeable in the B-BTMSH sample.

3.2.2. Nitrogen gas adsorption/desorption, bulk density and helium piconometry

Table 3 presents the bulk densities, porosities and BET specific surface areas of the synthesized aerogels. The bulk density for the sample made with the PEG additive (A-PEG) is lower than for the sample without PEG (A), proving that the PEG is partially removed during the washing before drying which leads to a decrease in the bulk density of the products. The specific surface area for the sample without PEG is higher than for the sample with PEG. These results are not in agreement with the obtained values for the bulk density, since the sample with PEG has a lower bulk density. This is certainly due to the residual additive retained in the pores of the sample, which leads to closed pores and, consequently, to a lower specific surface area. For the samples made in petri dishes, Table 3 shows that the sample made without additives presents better results in terms of bulk density. This means that the BTMSH and ODS lead to a higher degree of organization of the highly-random silica network derived from MTMS, which is due to the steric hindrance caused by the hexyl or octadecyl groups during gelation. The specific surface areas for these samples are similar and quite high ($> 320 \text{ m}^2 \text{ g}^{-1}$).

All the samples also exhibit high porosity ($> 94\%$), being A-PEG the sample with lowest bulk density and consequently highest value of porosity.

It is worth mentioning that the five aerogels presented type IV isotherms, usually obtained for mesoporous materials, with the typical hysteresis loop in the adsorption/desorption cycle. However, as seen in SEM images (Fig. 2), all types of pores are present in the aerogels structure; the different size of pores can be observed in Fig. 3 that shows the pore size distribution curves for all the samples.

Table 4

TGA results: thermal phenomena, characteristic temperatures and weight losses for the MTMS-derived aerogels with and without additives.

Sample	T_{onset} (°C)	T_{end} (°C)	Weight loss (%)	Source of weight losses
A	177	219	2.1	Evaporation/degradation of residual solvent/catalysts/water
	681	796	13.7	Thermal degradation of methyl groups overlapped with removal of structural OH groups
	186	227	4.2	Evaporation/degradation of residual solvent/catalysts/water
	303	405	2.3	Removal of structural OH groups and degradation of residual PEG
	551	644	5.9	1st stage of thermal degradation of methyl groups
	748	799	8.8	2nd stage of thermal degradation of methyl groups
B	169	214	1.5	Evaporation/degradation of residual solvent/catalysts/water
	327	429	3.4	Removal of structural OH groups
	516	602	4.9	1st stage of thermal degradation of methyl groups
	741	795	9.6	2nd stage of thermal degradation of methyl groups
B-BTMSH	186	223	0.5	Evaporation/degradation of residual solvent/catalysts/water
	373	456	2.8	Removal of structural OH groups
	544	568	2.3	1st stage of thermal degradation of methyl and hexyl groups
	718	797	6.7	2nd stage of thermal degradation of methyl and hexyl groups
B-ODS	188	227	3.6	Evaporation/degradation of residual solvent/catalysts/water
	496	569	24.2	Removal of structural OH groups overlapped with the octadecyl and methyl groups' thermal degradation
	745	798	8.4	2nd stage of thermal degradation of the alkyl groups

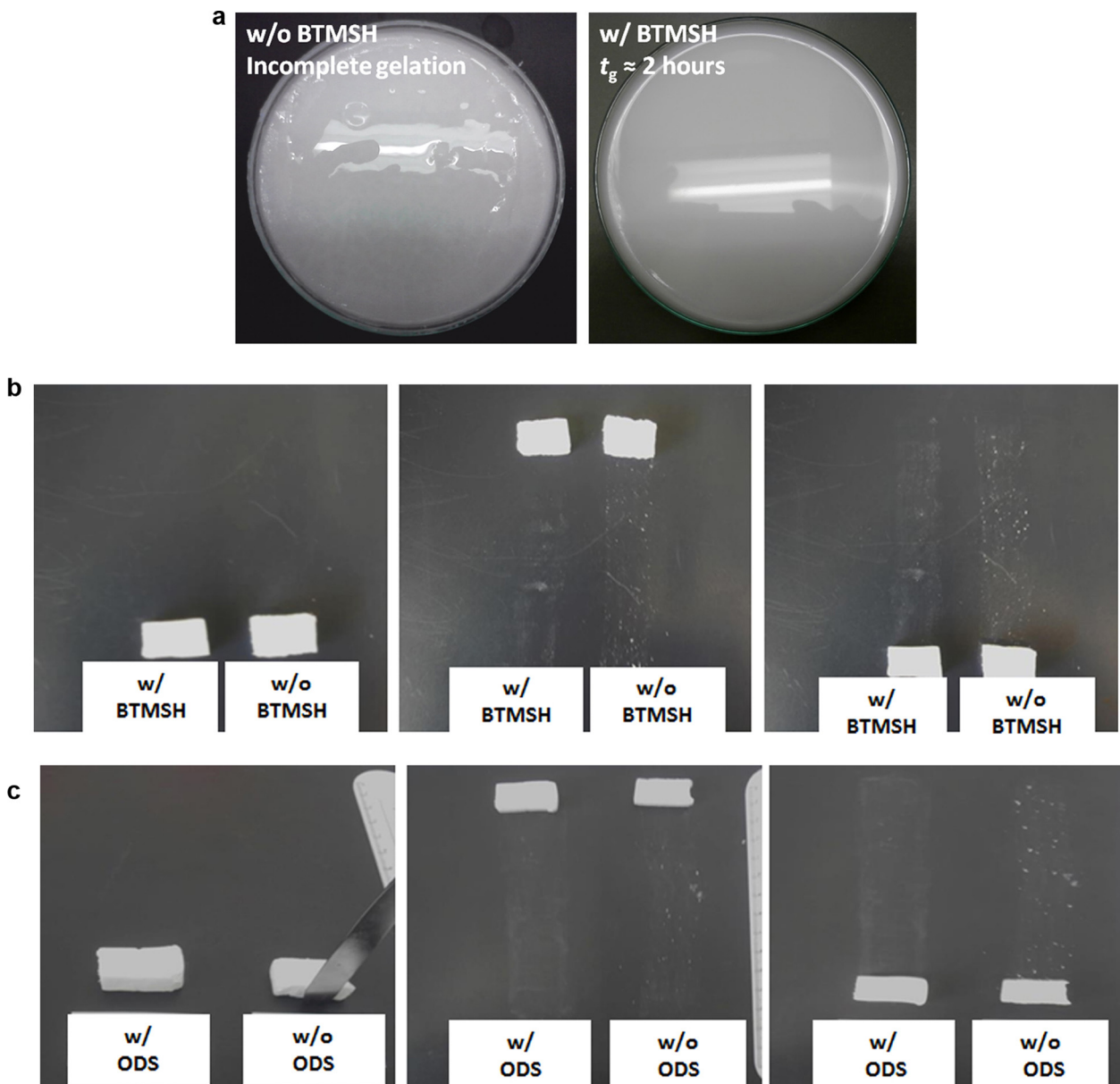


Fig. 4. (a) Gelation in Petri dishes with and without BTMSH additive, using a solvent/MTMS molar ratio of 35 and an acid solution concentration of 0.01 (t_g – gelation time); (b) Release of powders from the samples synthesized with BTMSH modifier; (c) Release of powders from the samples synthesized with ODS modifier.

The aerogels show an increase of pore volume approaching the boundary of micropores (2 nm), confirming a high amount of micropores in these materials. Except for sample B-ODS, they show a peak of pore volume in the region between 3 and 4 nm, which corresponds to mesopores. At higher pore sizes (mesopores and part of macropores), the samples show a broad peak that goes from 10 to 100 nm, and this peak has an increasing significance in the following order: A-PEG, B-BTMSH, B, A, B-ODS.

Comparing the samples A and B, they show similar patterns but the later has less meso and macropores, which is in agreement with its higher bulk density. The curve obtained for the sample made with the PEG additive shows that the addition of PEG600 (compare with sample A) leads to an aerogel structure with higher amount of small mesopores and lower amount of large mesopores, but a final apparent increase of the macropores. Thus, PEG gives some uniformity to the porous network. The aerogel containing BTMSH (B-BTMSH) shows a regular and low amount of mesopores and macropores between 4 and 90 nm and the highest peak at 3–4 nm. Also this additive, as PEG, contributes to some organization of the porous network, as can be confirmed in the SEM micrograph for this sample (Fig. 2).

The sample made with ODS has higher amount of meso and macropores and does not show the peak at 3–4 nm, revealing that ODS induces the formation of large pores, which was expected due to the high steric hindrance caused by octadecyl groups during gelation.

3.3. Thermal characterization

3.3.1. Thermal conductivity

The thermal conductivities, at three different temperatures, for the aerogels made with and without the additives are given in Table 3. The values of thermal conductivity demonstrate that these aerogels have a satisfactory insulation performance at room temperature ($0.036\text{--}0.039\text{ W m}^{-1}\text{ K}^{-1}$) and it clearly improves at low temperature (-25°C), which is an important feature for most Space environments. It should be noted that these measurements were carried out at atmospheric pressure and the thermal conductivity remarkably decreases in vacuum condition; this condition can positively affect the insulation performance of aerogels in Space. Results of Table 3 also show that the presence of additives does not deteriorate and in some cases improves the insulation performance of the aerogels, which may be due either to the increase of porosity and/or to a decrease of the proportion of large pores to small pores that decreases the gaseous component of the thermal conductivity. As expected, the thermal conductivity increases at higher temperatures.

3.3.2. TGA

The TGA weight losses of the aerogels and the underlying thermal phenomena that justify their occurrence are presented in Table 4. Due to the insulation character of these materials, the thermal degradation of alkyl groups frequently occurs in two stages, first in the more superficial groups and then extended to the more inner groups [15]. All the aerogels lose less than 5% of their mass (except sample A-PEG that loses 6.5 wt%) until $\sim 500^\circ\text{C}$, revealing high thermal stability of all the organically modified networks.

3.4. Mechanical characterization

The modulus of elasticity (Young's modulus) of the samples was determined by the slope of the initial linear portion of the stress-strain curve obtained during compression tests. It is possible to see that the additives, in the cases of PEG and ODS, can lead to a decrease in the modulus of elasticity and improve the flexibility of the materials (Table 3) when compared to the aerogels in the

same conditions without additive (samples A and B, respectively). Samples of type A reached a strain at break of $\sim 80\%$ and samples of type B achieved $\sim 70\%$, being the value for B-ODS the highest. The sample made with 2% of Si from ODS has better mechanical performance with a modulus of elasticity of only 3.1 kPa.

3.5. Visual inspection: gelation and dust release

Not less important are the results about the gelation time and the release of powders of the studied systems. It was possible to note, during this work, that the addition of BTMSH allowed improving the gelation, by increasing its extent and decreasing the gel time. This was particularly important in larger samples. Thus, with BTMSH, it was feasible to obtain homogeneous and cohesive gels in conditions of dilution in which it was impossible without this additive – Fig. 4a. In fact, with a MTMS/solvent molar ratio of 35 (image on the left), the gelation was incomplete without additive, showing some supernatant liquid and irregularities in the gel's surface. In this case, the gel gets destroyed only by the force of its own weight. The smooth and shiny surface of the gel with BTMSH (image on the right) is indicative of gel's consistency, homogeneity and strength.

Regarding the release of powders, the BTMSH and ODS additives have an expected effect of creating extra linking in the silica structure or reinforce it by the C18 alkyl chain, respectively. Thus, they are expected to increase the cleanliness of the aerogels. In this way, a fist test to evaluate the release of powders was performed, by subjecting samples of type B to an ultrasound vibration of 35 kHz during 30 min, inside a beaker placed in an ultra-sounds bath (Bandelin, Sonorex digiplus); this test did not prove to be effective and no released powder was detected, maybe due to very low weight of the samples and no fixation point. Thus, it was decided to observe the footprint of new samples of type B aerogels when pushed in a black paper as background contrast (see Section 2.2). By this second test, it was concluded that the addition of ODS and BTMSH to the sol gave rise to aerogels with less release of powders when compared to the reference sample B (Fig. 4b and c).

4. Conclusions

Monolithic silica aerogels were synthesized using MTMS as precursor and PEG, BTMSH and ODS as chemical additives in an attempt to obtain improved insulation materials.

The addition of PEG allowed obtaining samples with lower density, thermal conductivity and modulus of elasticity. The BTMSH promoted a good gelation of the samples. This result is very important to obtain samples of larger dimension. The ODS also gave rise to improved materials in terms of flexibility and thermal conductivity. In addition, both BTMSH and ODS reduces the release of powders, which is very convenient in many applications, particularly for Space technologies.

Acknowledgement

This work has received funding from the European Union's Seventh Framework Programme for research, technological development and demonstration under Grant Agreement No. 284494, under the scope of project AerSUS – Aerogel European Supplying Unit for Space Applications. Note that this work reflects only the authors' views, and the European Union is not responsible for any use that might be made of the content of the information contained in it.

References

- [1] S.M. Jones, J. Sakamoto, Applications of aerogels in space exploration, in: M.A. Aegerter, N. Leventis, M.M. Koebel (Eds.), *Aerogels Handbook*, Springer, New York, 2011, pp. 721–746.

- [2] H. Maleki, L. Durães, A. Portugal, An overview on silica aerogels synthesis and different mechanical reinforcing strategies, *J. Non-Crystalline Solids* 385 (2014) 55–74.
- [3] A.M. Anderson, M.K. Carroll, Hydrophobic silica aerogels: review of synthesis, properties and applications, in: M.A. Aegerter, N. Leventis, M.M. Koebel (Eds.), *Aerogels Handbook*, Springer, New York, 2011, pp. 47–77.
- [4] A.V. Rao, G.M. Pajonk, D.Y. Nadargi, M.M. Koebel, Superhydrophobic and flexible aerogels, in: M.A. Aegerter, N. Leventis, M.M. Koebel (Eds.), *Aerogels Handbook*, Springer, New York, 2011, pp. 79–101.
- [5] L. Durães, M. Ochoa, R. Patrício, N. Duarte, V. Redondo, A. Portugal, Effect of the drying conditions on the microstructure of silica based xerogels and aerogels, *J. Nanosci. Nanotechnol.* 12 (2012) 6828–6834.
- [6] T. Matias, M. Ochoa, A. Portugal, L. Durães, Influence of R and R' alkyl groups ($-CH_3$ or $-C_2H_5$) on the properties of aerogels synthesized from $RSi(OR')_3$ precursors, *Nano Stud.* 7 (2013) 145–160.
- [7] J. Martin, B. Hosticka, C. Lattimer, P.M. Norris, Mechanical and acoustical properties as a function of PEG concentration in macroporous silica gels, *J. Non-Cryst. Solids* 285 (2001) 222–229.
- [8] B. Tan, S.E. Rankin, Effects of progressive changes in organoalkoxysilane structure on the gelation and pore structure of templated and non-templated sol-gel materials, *J. Non-Cryst. Solids* 352 (2006) 5453–5462.
- [9] R. Brambilla, G.P. Pires, J.H.Z. Santos, M.S.L. Miranda, B. Chornik, Octadecylsilane-modified silicas prepared by grafting and sol-gel methods, *J. Electron. Spectrosc. Relat. Phenom.* 156–158 (2007) 413–420.
- [10] A.V. Rao, S.D. Bhagat, H. Hirashim, G.M. Pajonk, Synthesis of flexible silica aerogels using methyltrimethoxysilane (MTMS) precursor, *J. Colloid Interface Sci.* 300 (2006) 279–285.
- [11] A.M. Anderson, M.K. Carroll, E.C. Green, J.T. Melville, M.S. Bono, Hydrophobic silica aerogels prepared via rapid supercritical extraction, *J. Sol-Gel Sci. Technol.* 53 (2009) 199–207.
- [12] L. Durães, A. Moutinho, I. Seabra, B.F.O. Costa, H.C. Sousa, A. Portugal, Characterization of iron(III) oxide/hydroxide nanostructured materials produced by sol-gel technology based on the $Fe(NO_3)_3 \cdot 9H_2O - C_2H_5OH - CH_3CHCH_2O$ system, *Mater. Chem. Phys.* 130 (2011) 548–560.
- [13] R. Al-Oweini, H. El-Rassy, Synthesis and characterization by FTIR spectroscopy of silica aerogels prepared using several $Si(OR)_4$ and $R''Si(OR')_3$ precursors, *J. Mol. Struct.* 919 (2009) 140–145.
- [14] H.G.O. Becker, W. Berger, G. Domschke, E. Fanghänel, J. Faust, M. Fischer, F. Gentz, K. Gewald, R. Gluch, R. Mayer, K. Müller, D. Pavel, H. Schmidt, K. Schollberg, K. Schwetlick, E. Seiler, G. Zeppenfeld, *Organikum*, 2nd ed., Calouste Gulbenkian Foundation, Lisbon, 1997.
- [15] M. Ochoa, L. Durães, A.M. Beja, A. Portugal, Study of the suitability of silica based xerogels synthesized using ethyltrimethoxysilane and/or methyltrimethoxysilane precursors for aerospace applications, *J. Sol-Gel Technol.* 61 (2012) 151–160.